Cloudy Assessment within an Atmospheric Infrared Sounder Pixel by Combining Moderate Resolution Spectroradiometer and Atmospheric Radiation Measurement Program Ground-Based Lidar and Radar Measurements

L. Adhikari and Z. Wang
University of Wyoming
Laramie, Wyoming

D. Whiteman
National Aeronautics and Space Administration – Goddard Space Flight Center
Greenbelt, Maryland

Introduction

Water vapor is an important component of the atmosphere in terms of its effects on the global radiation budget through its interaction with both the terrestrial long wave radiation and short wave solar radiation through cloud formation. It is one of the most radiatively active constituent of the atmosphere, ranging from shortwave solar radiances through the broadband infrared (Soden and Bretherton 1993) to microwave region of the spectrum making it a major player in the global warming scenario (Ramanathan 1988; Cess et al. 1990). Its high temporal and spatial variation and large uncertainties associated with its retrieval are major challenges to computation of earth-atmosphere radiation balance and climate change.

Earth Observing System satellites have been providing valuable datasets on water vapor and temperature on a global scale. One of the major technological advancements in satellite retrieval of water vapor and temperature profiles have been achieved through the sounding suite aboard Earth Observing System AQUA. The sounding suite, whose major component is Atmospheric Infrared Sounder (AIRS), is expected to provide high quality temperature and moisture profiles. However, there are errors in the retrieval of water vapor in both clear and cloudy conditions and it inhibits the goals set for the sounding suite.

A new algorithm needs to be developed to address these retrieval issues. For the algorithm development, database with reliable temperature and water vapor profiles and cloudy assessment is important. Accurate cloud cover assessment of the AIRS footprint is essential to better characterize the retrieval algorithm.

The cloudy assessment is carried with collocated Moderate Resolution Spectroradiometer (MODIS) data and ground-based radar and lidar data. AIRS has a coarse spatial resolution so high spatial MODIS measurements can better characterize the sub-pixel level cloudy condition in the AIRS footprint (Li et al. 2004).

In the present study, a collocation algorithm has been developed that collocates the MODIS pixels within the AIRS footprints. The algorithm has been validated by comparing collocated AIRS and MODIS brightness temperatures. Collocated brightness temperatures at the infrared window channels centered at 11.06 and 11.03 microns for AIRS and MODIS respectively are compared. Current cloud fraction retrieval are compared for MODIS and AIRS to see their performance. These are validated using Atmospheric Radiation Measurement (ARM) Micro Pulse Lidar (MPL).

Collocation of AIRS and MODIS Footprints

The collocation algorithm uses the scanning geometry of the instruments to collocate the two sets of footprints with varying spatial resolutions. The AIRS instrument is a continuously operating cross-track scanning radiometer that scans from - 48.95º on the left side to 48.95º on the right side from the nadir (Aumann et al. 2003). During the cross-track scanning period, it produces 90 integration periods resulting in 90 cross-track footprints. The footprints are circular at nadir and elliptical away from the nadir. Both the shape and size thus change with the scanning angle of the instrument. The length of the major axis of the footprint varies from about 13.5 km at nadir to 31.3 km at the extreme scanning angles on either ends. The change in the minor axis is relatively small in comparison to the major axis. It varies from 13.5 km at nadir to 20.8 km at the two extreme ends.

Each AIRS footprint is formed by 1.1º angle beam. This makes the scanning angle at the two ends along the scanning direction to be $\theta + 0.55$ and $\theta - 0.55$ degrees, where θ is the scanning angle of the instrument. The footprints closest to the nadir are made by angles 0º and 1.1º on the right side of the nadir and by -1.1º and 0º on the left side of the nadir. This relates to the diameter along the scanning direction given by

$$D_x = h\,|\tan(\theta + 0.55) - \tan(\theta - 0.55)|,$$

where D_x is the diameter of the footprint along the scanning direction and h is the satellite altitude.

The length of the chord (l) across the scanning direction is calculated by using finite points along the diameter D_x as

$$l = 2h\,(\tan\,(\theta_2 - \theta_1)i/n)/\cos(\theta_1 + (\theta_2 - \theta_1)i/n)$$

where θ_2 and θ_1 are the scanning angle at the point along the diameter AB closest and farthest to the nadir respectively.

n and i are the total number of points taken along the diameter AB and its position in relation to point the closest point of the footprint from nadir respectively such that $0 \leq i \leq n$.

Figure 1 shows the collocated MODIS pixels within the AIRS footprints at the left end, center and the right end of the scanning direction respectively.

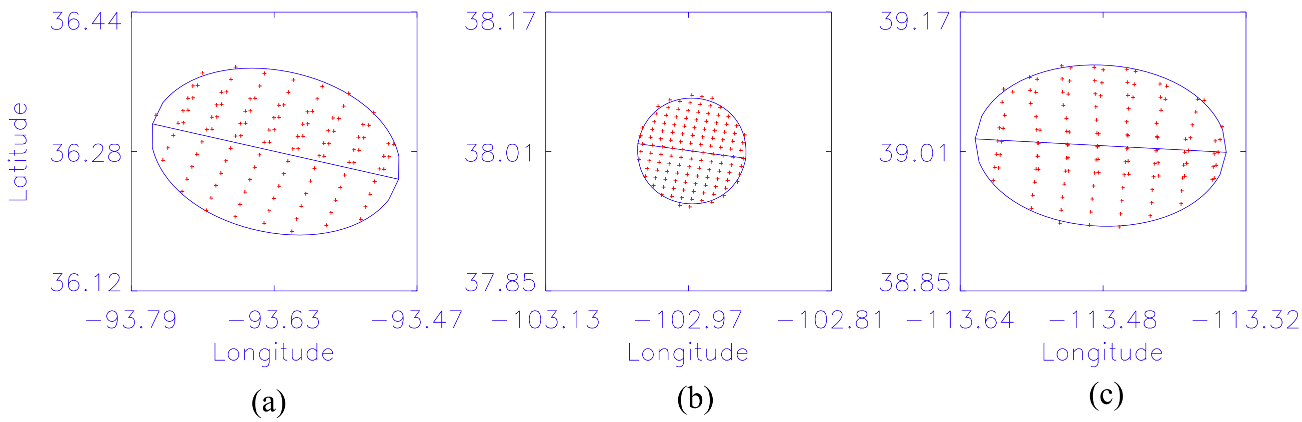

Figure 1. Collocated MODIS footprints within AIRS for (a) right-end (b) center and (c) left-end AIRS footprints.

Regression of brightness temperatures measured by collocated AIRS and MODIS window channel at 11.06 and 11.03 microns respectively show correlation coefficient of more than 0.99 for both day time and night time scenes. The correlation coefficients are 0.998 for both daytime and nighttime scenes. Figure 2 shows the regression of collocated brightness temperatures with AIRS brightness temperature against MODIS brightness temperature. The regression shows negative bias of -2.56 and -2.72 K for AIRS in comparison to MODIS for day time and night time scenes respectively and slopes of 1.01 for both daytime and nighttime scenes. The high correlation coefficient and slopes of 1.01 are taken as proof for the collocation algorithm's performance.

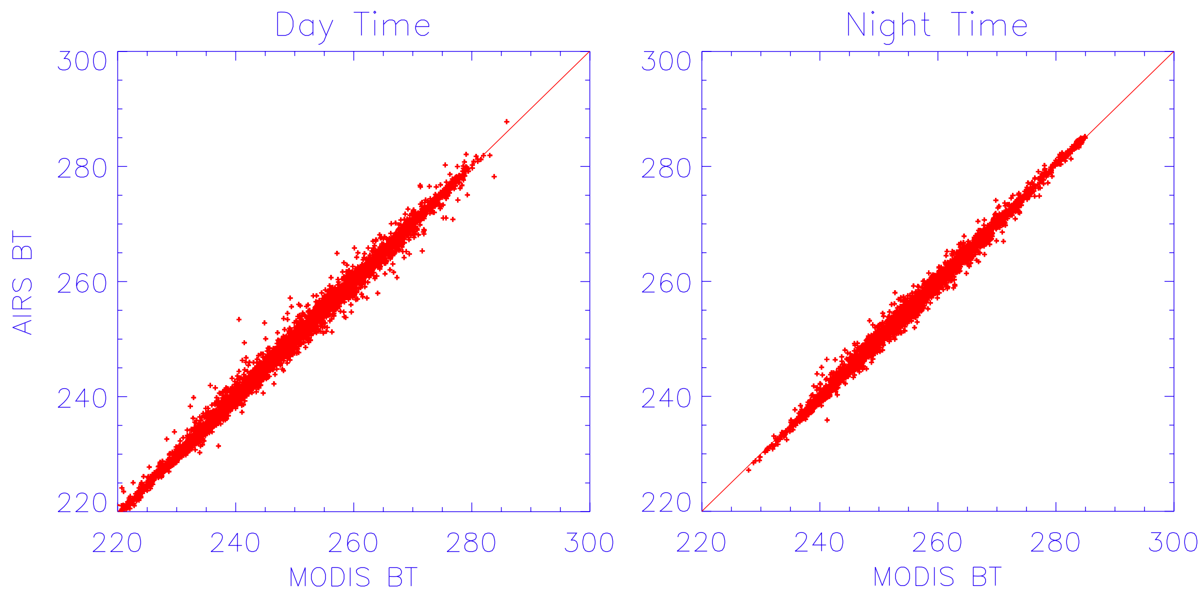

Figure 2. Regression of brightness temperature from collocated AIRS and MODIS.

Cloud Cover Comparison

A comparison of retrieved cloud fraction from AIRS and MODIS is presented. AIRS retrieved effective cloud cover, i.e., the product of fractional cloud cover and emissivity, is compared to MODIS retrieved cloud cover. Figure 3 shows the retrieved cloud cover from AIRS and MODIS. AIRS retrieved cloud fraction is measured for a bin size of 0.04 of MODIS retrieved cloud fraction. The figure shows the mean AIRS cloud fraction and the associated standard deviation for each of the bin sizes. The vertical bars represent the standard deviation from the mean value. In the low cloud cover cases, the AIRS tends to retrieve more cloud cover than MODIS and in higher cloud cover scenario, AIRS underestimates in relation to MODIS. When cloudy and probably cloudy scenes are taken from the MODIS cloud mask (Figure 3b), the underestimation in the AIRS retrieved cloud fraction is more pronounced with relation to MODIS retrieved cloud fraction.

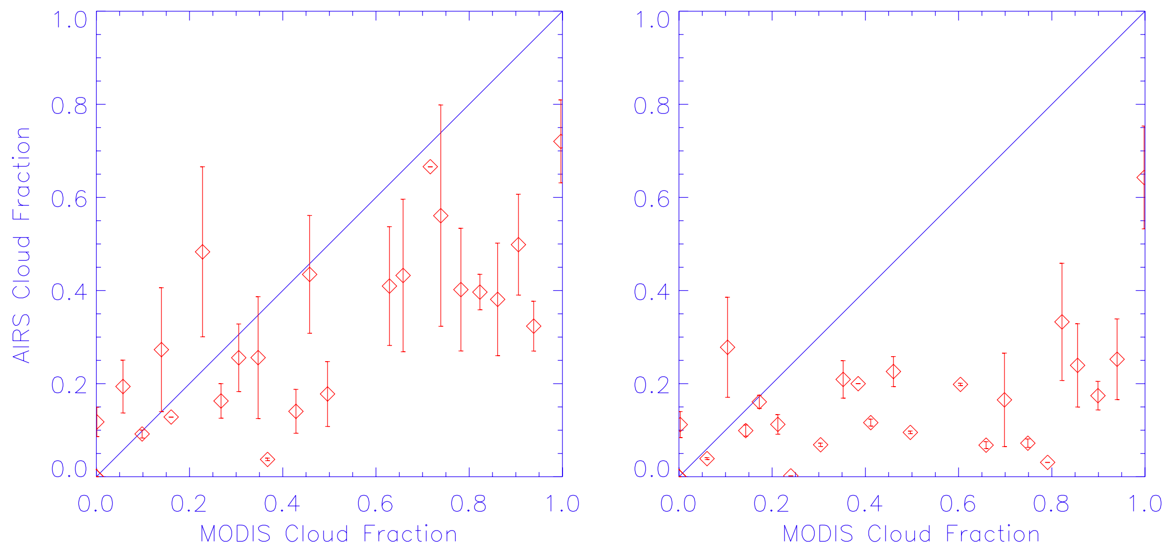

Figure 3. AIRS cloud fraction and standard deviation (vertical lines) with collocated MODIS cloud fraction using (a) MODIS cloud mask confident cloudy (b) sum of confident cloudy and probably cloudy scenes.

Both AIRS and MODIS have ambiguities in the retrieval of fractional cloud cover. A case study of completely clear day and completely overcast day is presented here. On the clear day, MODIS clearly indicates no cloud cover whereas AIRS shows 78% low cloud cover. On the overcast day, AIRS show two layer clouds covering the whole sky and MODIS only shows 36% cloud cover. Table 1 shows the two cases. Conf Cld represents cloud fraction obtained from MODIS cloud mask using confident cloudy scenes and total represent the sum of confident cloudy and probably cloudy scenes.

Table 1. Cloud Fractions retrieved from MODIS and AIRS.

		MODIS Cloud Fraction (%)		AIRS Cloud Fraction (%)	
Day	**Time**	**Conf Cld**	**Total**	**Upper**	**Lower**
May 29, 2003	0805	0	2	0	78
July 8, 2003	0855	36	100	78	22

The validation of the retrieved cloud fractions is done by using ARM MPL data. Figure 4 shows the clouds retrieved from the ground based MPL. It shows that May 29, 2003 is a clear day and multilayer clouds are present on July 8, 2003.

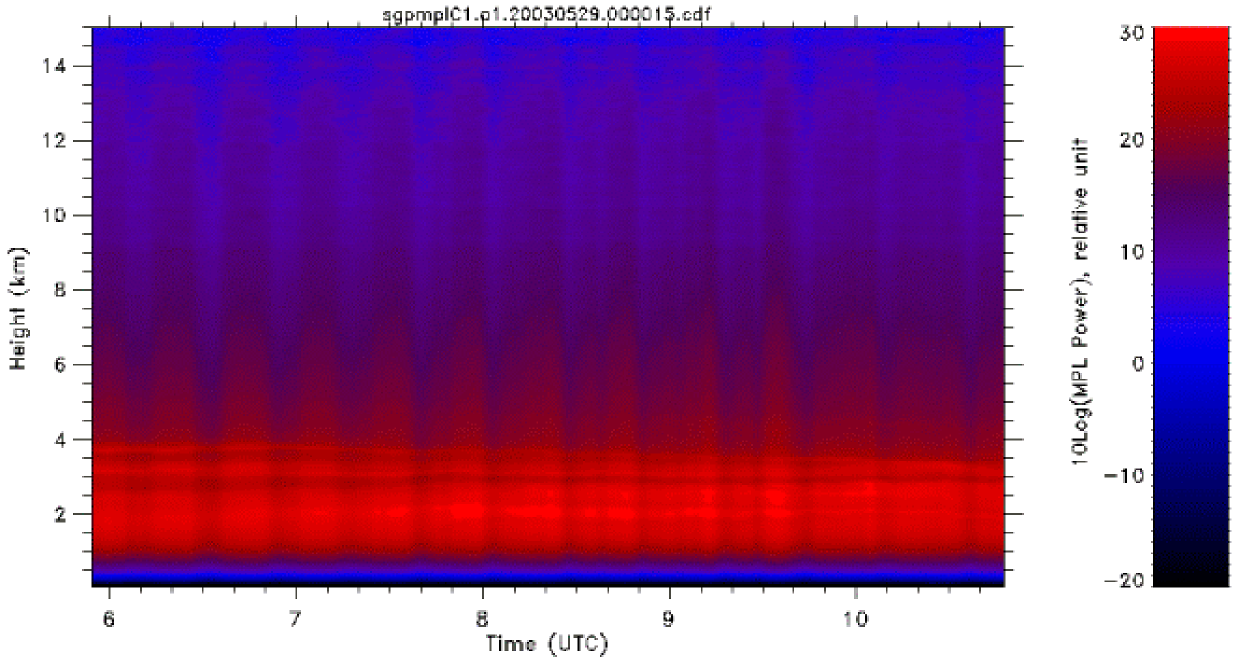

(a)

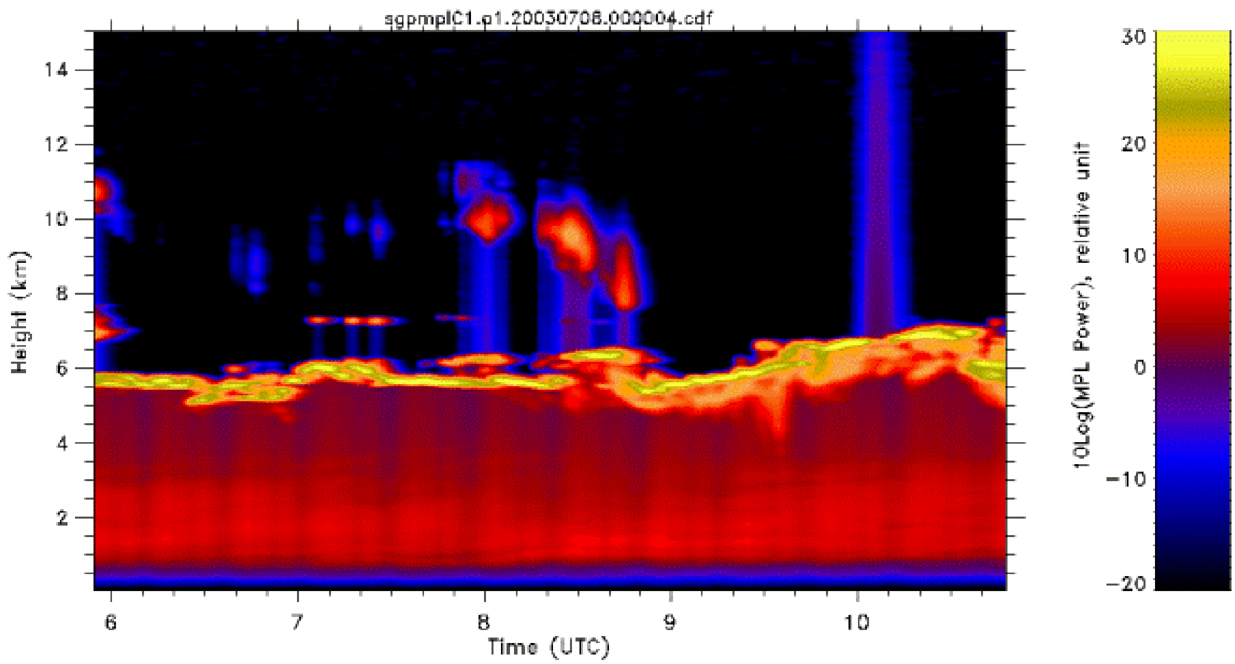

(b)

Figure 4. MPL data from ARM Southern Great Plains site for (a) May 29, 2003 and (b) July 8, 2003

Summary

MODIS cloud mask has a better spatial resolution so collocated MODIS cloud mask within the coarser spatial resolution AIRS would provide a better assessment of the cloud cover information within the AIRS footprint. As MODIS cloud detection also has some ambiguities, these can be reduced by using ground based lidar and radar data to improve MODIS cloud detection.

The algorithm for collocating MODIS within AIRS footprints give a high correlation coefficient for measured brightness temperatures indicating that the algorithm is satisfactory.

Conclusion and Further Work

The regression analysis on the IR brightness temperatures of collocated AIRS and MODIS gives a correlation coefficient of more than 0.99 for both clear and cloudy cases.

Bit-wise interpretation of MODIS cloud mask is required to identify clouds using MODIS.

Further work include application of the collocation algorithm to provide sub-pixel level cloud cover within the AIRS pixel around the ARM Southern Great Plains site using MODIS measurements and use ground-based lidar and radar measurements to improve the MODIS cloud detection.

Acknowledgment

Data were obtained from the ARM Program sponsored by the U.S. Department of Energy, Office of Science, Office of Biological and Environmental Research, Environmental Sciences Division.

Contact

Loknath Adhikari, Department of Atmospheric Science, University of Wyoming, Laramie, Wyoming 82071, Email: loknath@uwyo.edu

References

Aumann, HH, MT Chahine, C Gautier, MD Goldberg, E Kalnay, LM McMillin, H Revercomb, PW Rosenkranz, WL Smith, DH Staelin, LL Strow, and J Susskind. 2003. "AIRS/AMSU/HSB on the Aqua mission: Design, science objectives, data products, and processing systems." *IEEE Transactions on Geoscience and Remote Sensing* 41:253-264

Cess, RD, GL Potter, JP Blanchet, GJ Boer, AD Del Genio, M Deque, V Dymnikov, V Galin, WL Gates, SJ Ghan, JT Kiehl, AA Lacis, H Le Treut, Z-X Li, X-Z Liang, BJ McAvaney, VP Meleshko, JFB Mitchell, J-J Morcrette, DA Randall, L Rikus, E Roeckner, JF Royer, U Schlese, DA Sheinin, A Slingo, AP Sokolov, KE Taylor, WM Washington, RT Wetherald, I Yagai, and M-H Zhange. 1990. "Intercomparison and interpretation of climate feedback processes in 19 atmospheric general circulation models." *Journal of Geophysical Research* 95:16601-16615.

Li, J, WP Menzel, F Sun, TJ Schmmit, and J Gurka. 2004. "AIRS subpixel cloud characterization using MODIS cloud products." *Journal of Applied Meteorology* 43:1083-1094.

Ramanathan, V. 1988. "The greenhouse theory of climate change: A test by an inadvertent global experiment." *Science* 240:293-299.

Soden, BJ, and FP Bretherton. 1993. "Upper tropospheric relative humidity from GOES 6.7 µm channel: Method and climatology for July 1987." *Journal of Geophysical Research* 98:16669-16688.